Electronic Supplementary Material (ESI) for New Journal of Chemistry.

Subsurface and solid solution-type defect engineering in the $CoCr_2O_4$-Bi_2WO_4-NiS_2 nanocomposite for the visible light degradation of doxycycline and removal of chromium and its genotoxic evaluation in *Allium cepa*

S. Balasurya[a], Mohammad K. Okla[b], Saud S. Al-amri[b], Ibrahim A. Alaraidh[b], Abdullah A. Al-ghamdi[b], Walid Soufan[c], Mostafa A. Abdel-Maksoud[b,**], Ramadan F abdelaziz[d], Christian R. Studenik[d], S. Sudheer Khan[e,*]

[a]Nanobiotechnology Laboratory, Department of Biotechnology, Bannari Amman Institute of Technology, Sathyamangalam, Tamil Nadu, India.
[b]Botany and Microbiology Department, College of Science, King Saud University, P.O. Box 2455, Riyadh 11451, Saudi Arabia

[c]Plant Production Department, College of Food and Agriculture Sciences, King Saud University, P.O. Box 2460, Riyadh 11451, Saudi Arabia.

[d]Department of Pharmaceutical Sciences, Division of pharmacology and Toxicology, University of Vienna, Austria.

[e]Department of Oral Medicine and Radiology, Saveetha Dental College and Hospitals, Saveetha Institite of Medical and Technical Sciences (SIMATS), Chennai- 600077, Tamil Nadu, India.

*Corresponding author

Dr. S. Sudheer Khan

Email: sudheerkhans.sdc@saveetha.com

**Co-corresponding author

Dr. Mostafa A. Abdel-Maksoud

Email: harrany@gmail.com

Text S1. Characterization

The formation heterogeneous structure of $CoCr_2O_4$-Bi_2WO_4-NiS_2 NC was confirmed by XRD pattern, which determines the purity and crystalline nature of the prepared particle (Bruker D8 Advance, Germany). The morphology structure of the $CoCr_2O_4$-Bi_2WO_4-NiS_2 NC was determined by transmission electron microscopy (TEM, carl-Zeiss, Germany). The morphology structure of the $CoCr_2O_4$-Bi_2WO_4-NiS_2 NC was determined by transmission electron microscopy by field emission scanning electron microscopy (FESEM, JEOL, Japan). The elemental analysis of the prepared particle was determined by FE-SEM coupled with Energy-dispersive X-ray spectroscopy (EDS). Fourier-transform infrared spectroscopy (FTIR) data was used to determine the vibrational stretching present in the synthesized particle. S. Brunauer, P. Emmett, and E. Teller (BET) surface area analyzer (Thermo Fisher Scientific Nicolet IS50) was used to determine the surface area and porous nature of the materials. UV-visible diffusion reflection spectroscopy (DRS) of the $CoCr_2O_4$-Bi_2WO_4-NiS_2 was used to determine the reflection spectra of the prepared particle (Perkin–Elmer Lambda 750). The effective charge separation of the nanomaterial was characterized by photoluminescence spectroscopy (PL) and electrochemical impedance spectroscopy (EIS). The X-ray photoelectron spectroscopy was analyzed by using Physical Electronics (PHI Versa Probe III) to determine the chemical composition and to confirm the formation of $CoCr_2O_4$-Bi_2WO_4-NiS_2 NC.

Fig. S1. (a) UV- visible diffusion reflectance spectra, (b) EIS and (c) BET isotherm of $CoCr_2O_4$, Bi_2WO_6, NiS_2 and $CoCr_2O_4$-Bi_2WO_6-NiS_2 NC.

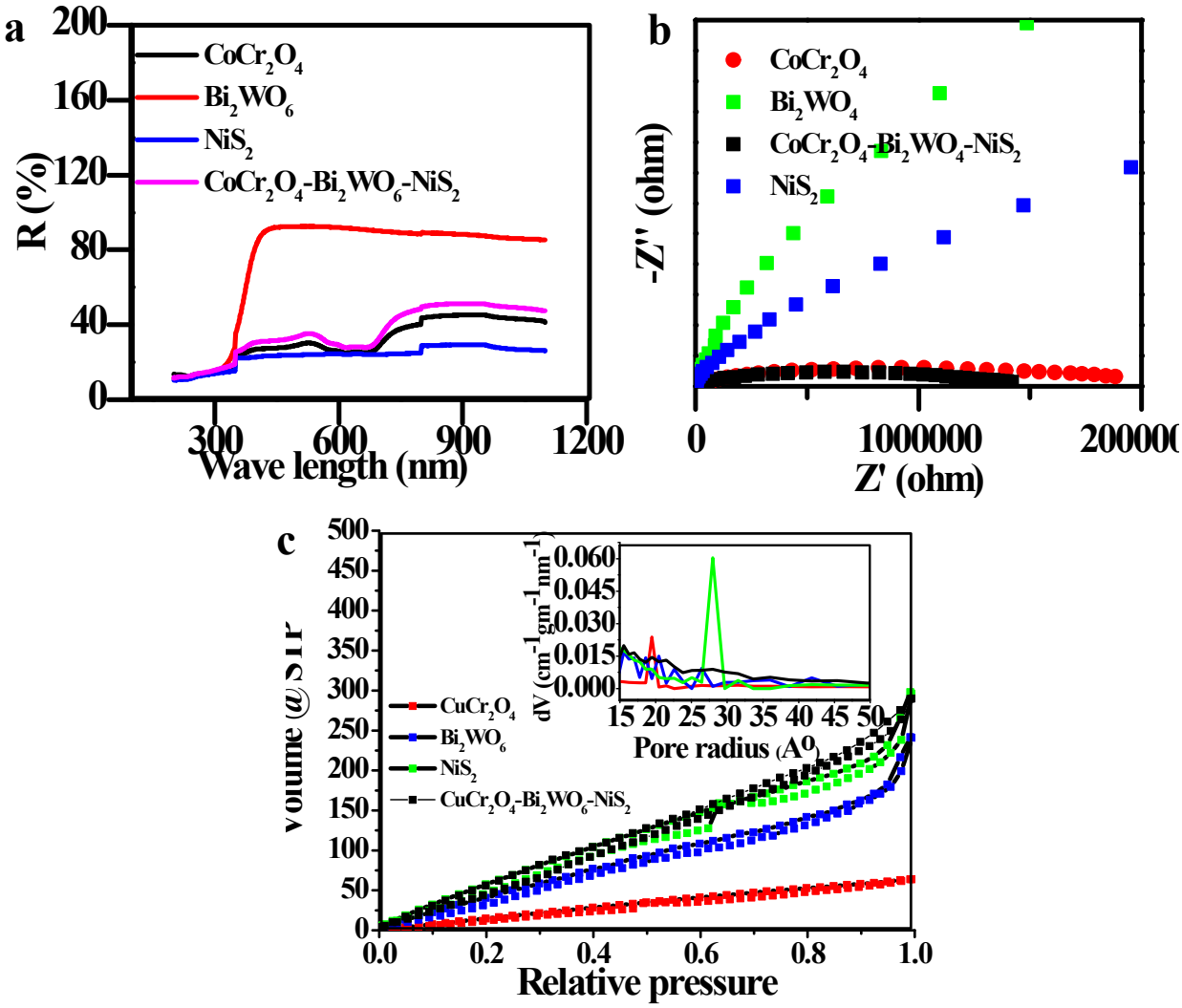

Fig. S2. Plot of C/C_0 and $\ln(C/C_0)$ vs time at (a1 & a2) different pH, (b1 & b2) at different concentration of NCs and (c1 & c2) at different concentration of doxycycline (doxy).

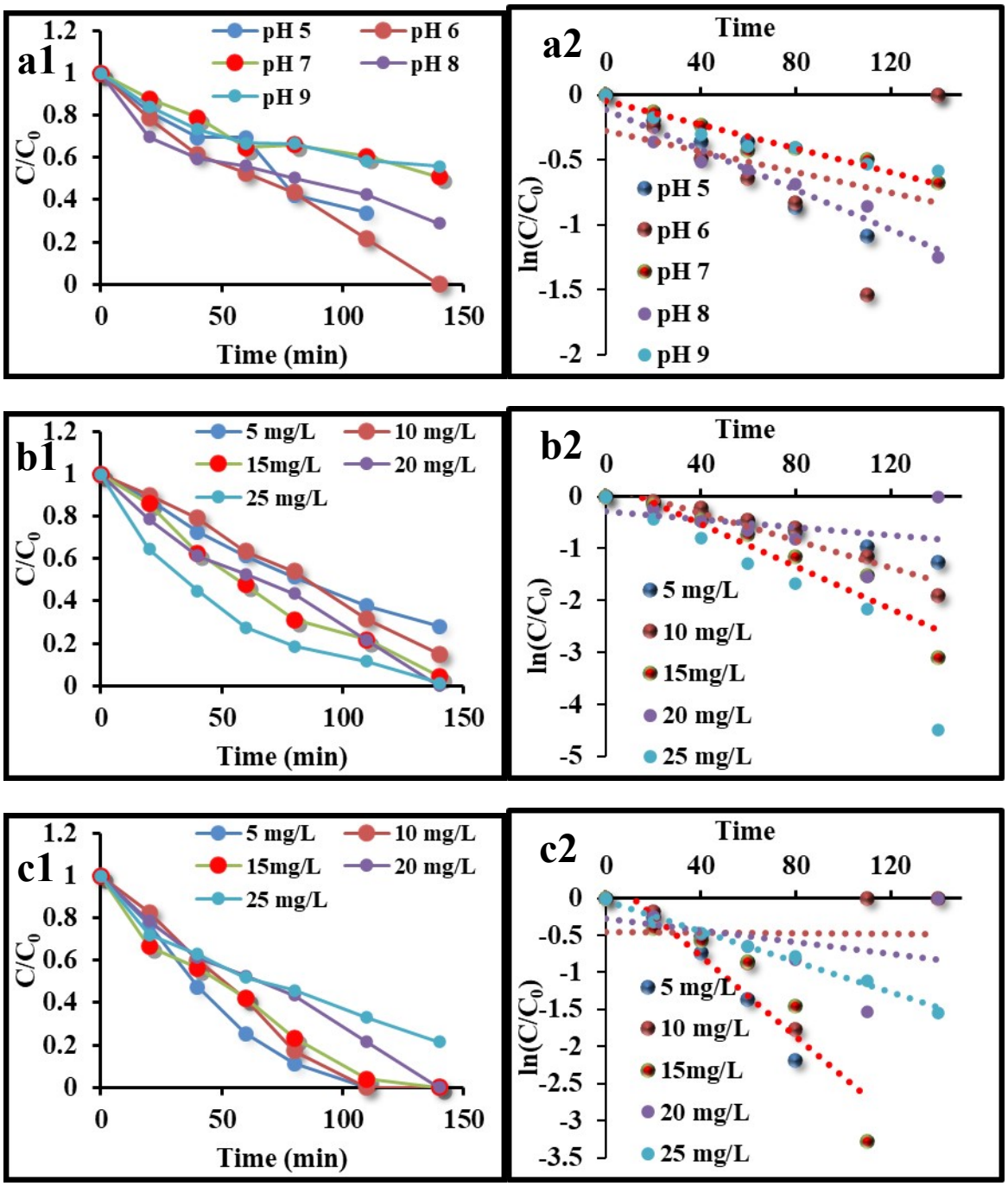

Fig. S3. Plot of C/C_0 and $\ln(C/C_0)$ vs time (a1 & a2) at different pH, (b1 & b2) at different concentration of NCs and (c1&c2) at different concentration of Cr(VI).

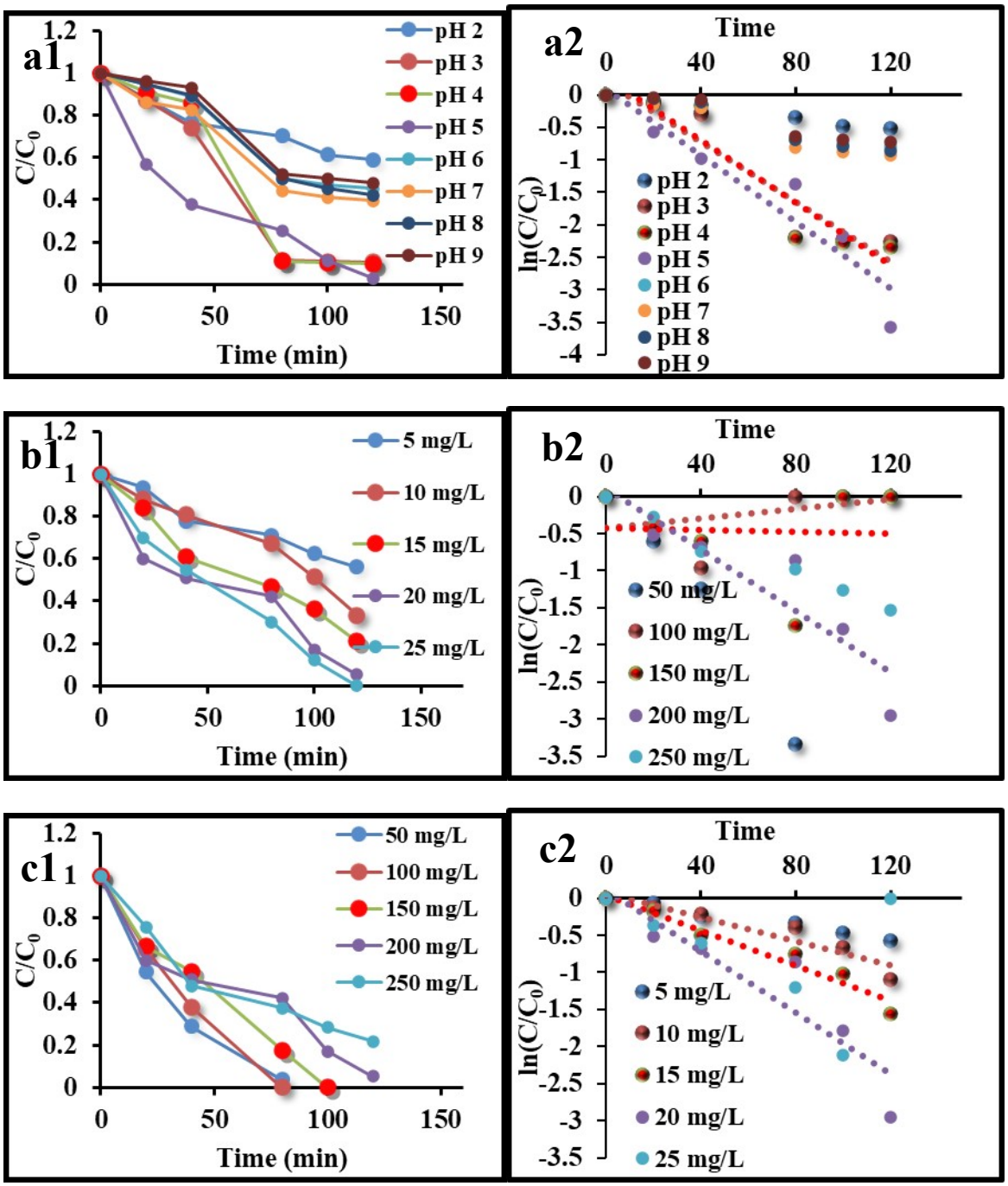

Fig. S4. Reusability on the photocatalytic degradation of doxy (a1) and photocatalytic removal of Cr(VI) (a2),scavenging on the photocatalytic degradation of doxy (b1) and photocatalytic removal of Cr(VI) (b2), (c) ESR of NC and XRD of NC before and after degradation.

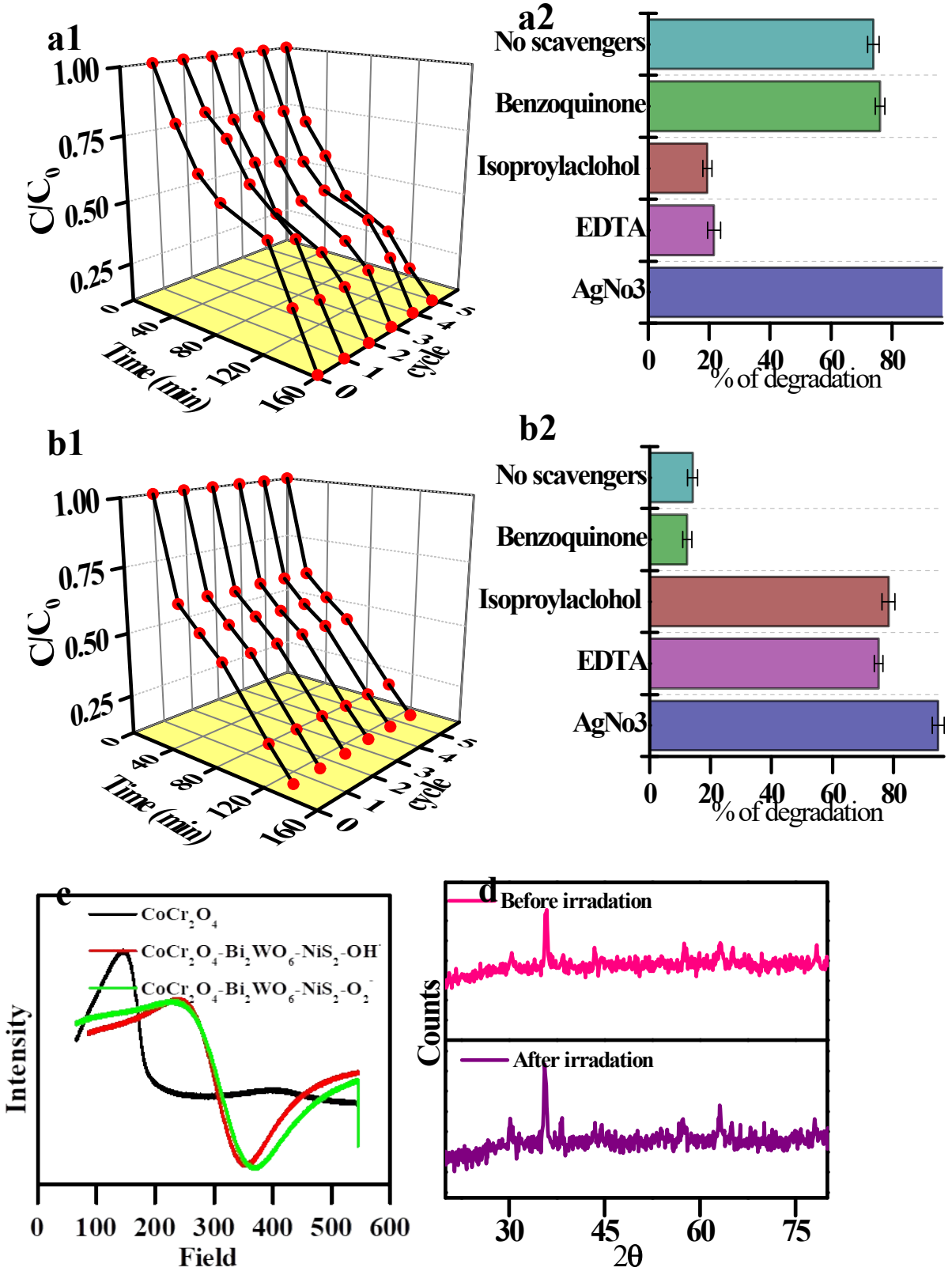

Fig.

Fig. S5. Electronic band structure and DOS of (a) $CoCr_2O_4$, (b) $Bi_2WO_6$and (c) NiS_2 NPs.

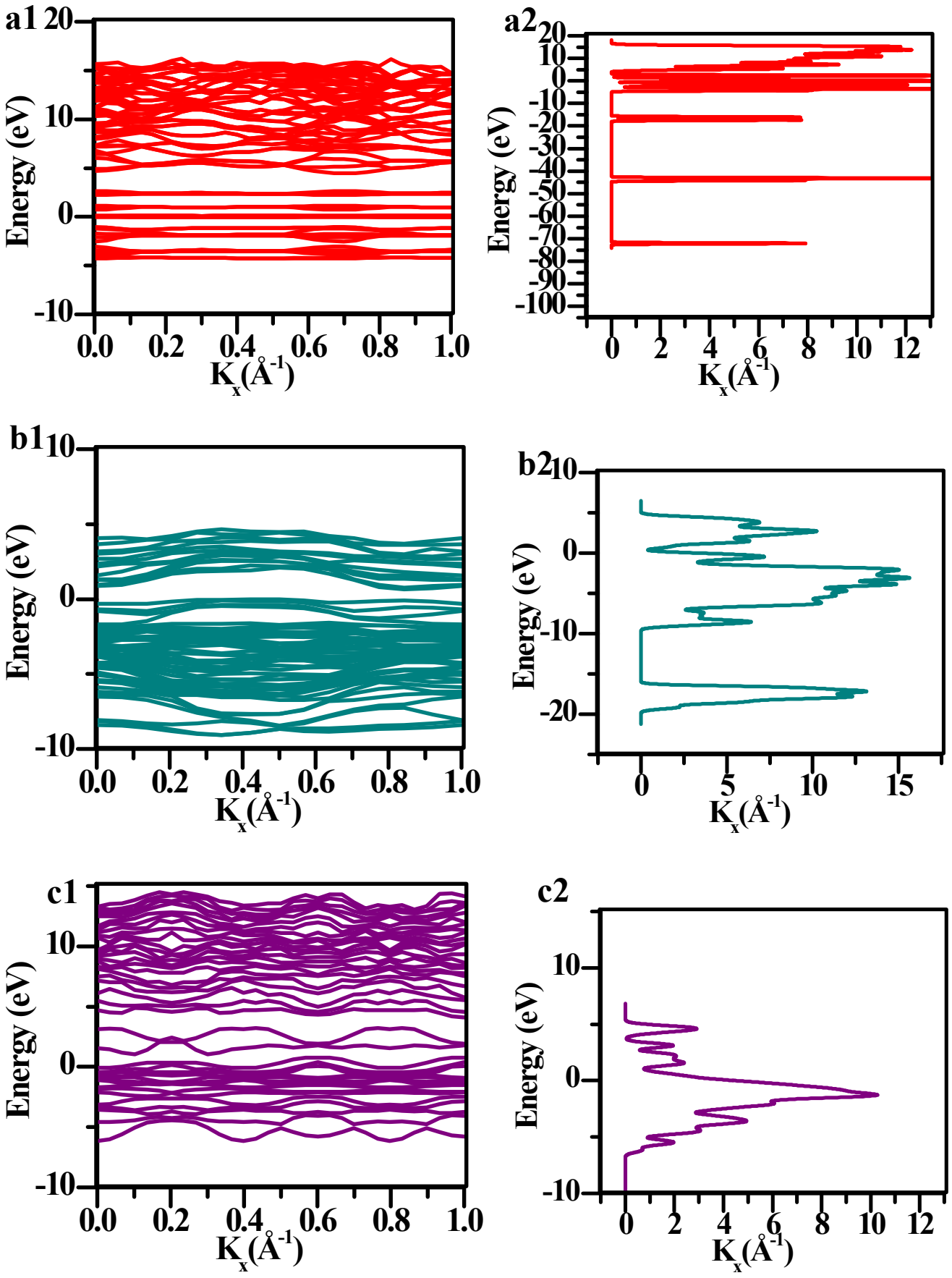

Table S1. BET surface areas, pore volume and pore size values of the prepared samples.

Sample	Specific surface area (m^2/g)	Average pore diameter (nm)	Pore volume (cm^3/g)
$CoCr_2O_4$	61.3	3.8	0.095
Bi_2WO_6	162.8	3.2	0.335
NiS_2	215.9	2.7	0.439
$CoCr_2O_4$-Bi_2WO_6-NiS_2	246.7	3.2	0.43

Table S2. Fukui function of Doxycycline

	F(0)	F(+)	F(-)
O1	0.014	0.014	0.014
O2	0.012	0.028	-0.003
O3	0.033	0.062	0.005
O4	0.017	0.012	0.021
O5	0.041	0.065	0.018
O6	0.034	0.026	0.041
O7	0.02	0.03	0.01
O8	0.027	0.027	0.026
N1	0.102	-0.002	0.205
N2	0.017	0.01	0.023
C1	0	0	0.001
C2	0.003	0.003	0.002
C3	0.002	0.001	0.003
C4	0.002	0.008	-0.003
C5	0.01	0.002	0.018
C6	0.002	0.003	0.001
C7	0.014	0.027	0.001
C8	0.033	0.074	-0.009
C9	0.002	-0.003	0.006
C10	0.014	0.03	-0.002
C11	0.001	0.005	-0.002
C12	0.043	0.076	0.01
C13	0.011	0.02	0.002
C14	0.008	0.016	0
C15	0.006	0.009	0.004
C16	0.017	0.029	0.006
C17	0.022	0.003	0.041
C18	0.023	0.005	0.041
C19	0.02	0.032	0.008
C20	0.006	0.006	0.006
C21	0.038	0.062	0.015
C22	0.022	0.033	0.012
H1	0.006	0.006	0.006
H2	0.008	0.014	0.002
H3	0.004	0.002	0.007
H4	0.031	0.009	0.052
H5	0.008	0.013	0.003

H6	0.005	0.005	0.005
H7	0.009	0.017	0.002
H8	0.011	0.013	0.009
H9	0.008	0.011	0.006
H10	0.012	0.012	0.013
H11	0.014	0.023	0.005
H12	0.019	0	0.038
H13	0.043	0.009	0.078
H14	0.023	0.011	0.035
H15	0.044	0.01	0.077
H16	0.017	0.002	0.031
H17	0.024	0.01	0.038
H18	0.008	0.008	0.008
H19	0.011	0.017	0.005
H20	0.022	0.033	0.011
H21	0.018	0.025	0.01
H22	0.007	0.003	0.011
H23	0.016	0.014	0.019
H24	0.015	0.022	0.009

Table S3. The occurrence of cytological defects in root cells per 1000 cells after treatment of *A. cepa* with different concentrations of $CoCr_2O_4/Bi_2WO_6/NiS_2$ nanocomposite.

Treatments	Sample size n=5	MI[a] (%)	P[b] (%)	M[c] (%)	A[d] (%)	T[e] (%)	Mean MI (%) ± SE
0 µg/mL	Sample 1	99.6	98.4	0.8	0	0.8	98.9±0.71
	Sample 2	98.7	98.6	0.4	0.4	0.6	
	Sample 3	97.8	98.4	0.6	0.2	0.8	
	Sample 4	99.4	97.9	0.3	0.7	1.1	
	Sample 5	99.1	98.2	1.1	0.3	0.4	
10 µg/mL	Sample 1	99.2	97.7	0.9	0.8	0.6	98.47±0.83
	Sample 2	99.1	98.3	0.6	0.7	0.4	
	Sample 3	98.9	97.9	0.4	0.6	1.1	
	Sample 4	97.9	97.2	1.2	0.9	0.7	
	Sample 5	97.3	96.9	1.3	0.9	0.9	
20 µg/mL	Sample 1	98.2	97.2	0.8	0.6	1.4	97.17±0.59
	Sample 2	96.9	98.4	0.1	1.4	0.1	
	Sample 3	97.2	97.2	0.9	0.8	1.1	
	Sample 4	96.7	96.9	0.8	0.7	1.6	
	Sample 5	96.9	97.2	1.1	0.6	1.1	
30 µg/mL	Sample 1	97.1	96.8	1.4	0.4	1.4	95.39±1.23
	Sample 2	96.2	96.3	1.1	0.9	1.6	
	Sample 3	94.1	95.8	0.9	1.4	0.9	
	Sample 4	95.1	96.2	0.1	0.7	1.1	
	Sample 5	94.5	95.2	0.8	0.9	0.4	
40 µg/mL	Sample 1	89.6	96.4	0.8	0.2	0.4	87.75±3.08
	Sample 2	92.1	94.6	0.6	0.9	0.7	
	Sample 3	86.2	95.3	1.2	0.2	0.7	
	Sample 4	84.2	96.1	0.6	0.8	1.4	
	Sample 5	86.9	91.9	0.4	0.8	1.1	
50 µg/mL	Sample 1	80.4	92.1	0.9	0.8	1.1	78.14±2.77
	Sample 2	81.6	93.4	0.8	0.6	0.8	
	Sample 3	74.9	92.6	1.4	0.2	0.9	
	Sample 4	76.4	96.7	1.2	0.4	1.1	
	Sample 5	77.6	93.4	0.6	0.4	1.1	

[a]Mitotic index, [b]Prophase, [c]Metaphase, [d]Anaphase, [e]Telophase

Table S4. Chromosomal aberrations and micro nuclei of root cells of *A. cepa* treated with different concentration of $CoCr_2O_4/Bi_2WO_6/NiS_2$ nanocomposite.

Concentration of ZnO NPs (µg/mL)	Sample size n-5	Chromosomal aberration				Chromosomal aberration index (%)	Chromosomal aberration				Micronuclei index(%)
		Defects in prophase	Defects in metaphase	Defects in anaphase	Defects in telophase		Defects in prophase	Defects in metaphase	Defects in anaphase	Defects in telophase	
0	S 1	-	-	-	-	Nil	-	-	-	-	Nil
	S 2	-	-	-	-		-	-	-	-	
	S 3	-	-	-	-		-	-	-	-	
	S 4	-	-	-	-		-	-	-	-	
	S 5	-	-	-	-		-	-	-	-	
10	S 1	-	-	-	-	Nil	-	-	-	-	Nil
	S 2	-	-	-	-		-	-	-	-	
	S 3	-	-	-	-		-	-	-	-	
	S 4	-	-	-	-		-	-	-	-	
	S 5	-	-	-	-		-	-	-	-	
20	S 1	-	-	-	-	Nil	-	-	-	-	Nil
	S 2	-	-	-	-		-	-	-	-	
	S 3	-	-	-	-		-	-	-	-	
	S 4	-	-	-	-		-	-	-	-	
	S 5	-	-	-	-		-	-	-	-	
30	S 1	-	-	-	-	0.9 ± 0.3	-	-	-	-	Nil
	S 2	-	+	-	-		-	-	-	-	
	S 3	+	-	-	-		-	-	-	-	
	S 4	-	-	-	-		-	-	-	-	
	S 5	-	-	+	-		-	-	-	-	
40	S 1	-	-	-	-	1.4± 0.8	-	-	-	-	Nil
	S 2	-	-	-	+		-	-	-	-	
	S 3	-	-	-	-		-	-	-	-	
	S 4	-	-	+	-		-	-	-	-	
	S 5	-	-	-	-		-	-	-	-	
50	S 1	-	-	-	-	2.1 ± 0.6	-	-	-	-	Nil
	S 2	+	-	-	-		-	-	-	-	
	S 3	-	-	+	-		-	-	-	-	
	S 4	-	+	-	+		-	-	-	-	
	S 5	-	-	+	-		-	-	-	-	